Phase transitions in supercritical explosive percolation

Wei Chen,[1,2,3,*] Jan Nagler,[4,5,†] Xueqi Cheng,[2] Xiaolong Jin,[2] Huawei Shen,[2] Zhiming Zheng,[6] and Raissa M. D'Souza[3,‡]

[1]*School of Mathematical Sciences, Peking University, Beijing, China*

[2]*Institute of Computing Technology, Chinese Academy of Sciences, Beijing, China*

[3]*University of California, Davis, California 95616, USA*

[4]*Max Planck Institute for Dynamics and Self-Organization (MPI DS), Göttingen, Germany*

[5]*Institute for Nonlinear Dynamics, Faculty of Physics, University of Göttingen, Göttingen, Germany*

[6]*Key Laboratory of Mathematics, Informatics and Behavioral Semantics, Ministry of Education, Beijing University of Aeronautics and Astronautics, 100191 Beijing, China*

(Received 9 January 2013; published 24 May 2013)

Percolation describes the sudden emergence of large-scale connectivity as edges are added to a lattice or random network. In the Bohman-Frieze-Wormald model (BFW) of percolation, edges sampled from a random graph are considered individually and either added to the graph or rejected provided that the fraction of accepted edges is never smaller than a decreasing function with asymptotic value of α, a constant. The BFW process has been studied as a model system for investigating the underlying mechanisms leading to discontinuous phase transitions in percolation. Here we focus on the regime $\alpha \in [0.6,0.95]$ where it is known that only one giant component, denoted C_1, initially appears at the discontinuous phase transition. We show that at some point in the supercritical regime C_1 stops growing and eventually a second giant component, denoted C_2, emerges in a continuous percolation transition. The delay between the emergence of C_1 and C_2 and their asymptotic sizes both depend on the value of α and we establish by several techniques that there exists a bifurcation point $\alpha_c = 0.763 \pm 0.002$. For $\alpha \in [0.6,\alpha_c)$, C_1 stops growing the instant it emerges and the delay between the emergence of C_1 and C_2 decreases with increasing α. For $\alpha \in (\alpha_c,0.95]$, in contrast, C_1 continues growing into the supercritical regime and the delay between the emergence of C_1 and C_2 increases with increasing α. As we show, α_c marks the minimal delay possible between the emergence of C_1 and C_2 (i.e., the smallest edge density for which C_2 can exist). We also establish many features of the continuous percolation of C_2 including scaling exponents and relations.

DOI: 10.1103/PhysRevE.87.052130 PACS number(s): 64.60.ah, 64.60.aq, 89.75.Hc, 02.50.Ey

I. INTRODUCTION

Percolation in networks, a phase transition from small, scattered components to large-scale connectivity, is heavily studied and widely applied in technological and social systems [1–4], biological networks [5,6], epidemiology [7–10], and even dynamical models of economic systems [11,12]. One of the most classic and widely studied models is the Erdös-Rényi random graph (ER) started from a collection of n initially isolated nodes, where edges sampled uniformly from the complete graph are sequentially added between nodes. Percolation under ER-like processes is considered a robust continuous phase transition with a unique giant component emerging at the percolation threshold [13]. Thus, altering the location and nature of the percolation phase transition has been a long-standing challenge. Three years ago, Achlioptas *et al.* proposed a modified ER model in which two random edges are sampled simultaneously but only the edge connecting two components with smaller product of their sizes is added while the other edge is discarded. The authors showed that the percolation transition can thus be delayed considerably, and when the transition eventually happens it is extremely abrupt, calling the phenomena "explosive percolation" [14]. They presented strong numerical evidence suggesting that the resulting percolation transition was, in fact, discontinuous. Many efforts were made to study similar processes on different topologies, showing that explosive percolation is observed in scale-free networks and lattices [15–19]. Although such explosive percolation phenomena resulting from the choice between a *fixed* number of random edges, as studied in [14], was later demonstrated to be actually *continuous* [20–24], several alternative models are now known to exhibit truly discontinuous percolation transitions [25–37].

Chen and D'Souza recently established [38] that the percolation transition is discontinuous for a stochastic graph evolution model introduced by Bohman, Frieze, and Wormald [39] (the BFW model) which examines a single edge at a time (rather than a model like that in [14], which examines multiple edges at each time step). Here, each edge is independently either added to the graph or rejected, provided that the fraction of accepted edges is never smaller than a decreasing function with asymptotic value of α, a constant. In [38] they showed that the BFW model exhibits a discontinuous percolation transition leading to the simultaneous emergence of multiple giant components, and that the number of stable giant components can be tuned via the parameter α. In [40] the underlying mechanism leading to the discontinuous phase transition was derived, namely that growth of the largest component is dominated by overtaking when two smaller components merge together to become the new largest component. Such growth by overtaking is a natural growth mechanism observed in many complex systems from ecologies to the business world [41–43]. Additionally, the discovery of

*chenwei2012@ict.ac.cn
†jan@nld.ds.mpg.de
‡raissa@cse.ucdavis.edu

 ©2013 American Physical Society

multiple giant component is unanticipated [44] and may have applications in polymerization [45], network discovery [46], and epidemiology [47].

The nature of explosive percolation phase transitions has been the topic of intense debate for the past few years [20–24,48], but more recently, we are learning that the evolution of such processes in the supercritical regime can also be unique and of great interest. For instance, in the supercritical regime, the size of the largest component can be a non-self-averaging quantity [49], furthermore, there can be multiple discontinuous jumps in the size of the largest component [50]. Here we investigate, both numerically and analytically, a generalized BFW model in the supercritical regime.

Specifically we study the initial percolation transition and supercritical evolution of the BFW model for the parameter $\alpha \in [0.6,0.95]$. (This regime is simplest, as only one giant component initially emerges in a discontinuous phase transition.) We show that the largest component eventually stops growing leading to the emergence of a second giant component at some delayed time, and that the second component is stable persisting throughout the subsequent evolution. Via an extensive finite size scaling analysis we establish that the second transition is continuous. The main result we derive is that there exists a critical value α_c such that, for $\alpha \in [0.6,\alpha_c)$.

C_1 stops growing at the discontinuous percolation transition, yet for $\alpha \in (\alpha_c,0.95]$, C_1 continues growing for some time into the supercritical regime, see Fig. 1(a). Furthermore, for $\alpha < \alpha_c$, the value of C_1 at percolation threshold becomes smaller with increasing α. As fewer edges are necessary to create a smaller C_1, this leads to enhanced growth of C_2 in the supercritical regime. Thus the gap between the two percolation transitions is smaller with increasing α for $\alpha < \alpha_c$. For $\alpha > \alpha_c$, in contrast, the value of C_1 at the time when it stops growing in the supercritical regime becomes larger with increasing α. As more edges are required to create a larger C_1, this leads to delayed growth of C_2. Thus the gap between the two percolation transitions is larger with increasing α for $\alpha > \alpha_c$. As we show, α_c marks the minimal delay possible between the emergence of C_1 and C_2 (i.e., the smallest edge density for which C_2 can exist).

The rest of the paper is organized as follows. In Sec. II we discuss the BFW model and show further evidence for the discontinuous transition of the largest component. In Sec. III, we analyze the growth cessation of the largest component in the supercritical regime. Section IV contains an analysis of the critical behavior of the second phase transition through finite size scaling. We conclude with some discussion in Sec. V.

II. THE BFW MODEL AND THE DISCONTINUOUS TRANSITION IN C_1

In this section, we illustrate the BFW model. The system is initialized with N isolated nodes and a cap, k, on the maximum allowed component size set to $k = 2$ and increased in stages as follows. Edges are sampled one at a time, uniformly at random from the complete graph. If an edge would lead to formation of a component of size less than or equal to k it is accepted. Otherwise the edge is rejected provided that the fraction of accepted edges remains greater than or equal to a function $g(k) = \alpha + (2k)^{-1/2}$, where α is a tunable parameter. (In the original BFW model, Bohman, Frieze, and Wormald only studied the case of $\alpha = 1/2$ and showed that the percolation threshold of this model is larger than 0.966 89) Finally, if the fraction of accepted nodes would drop below $g(k)$, the cap is augmented to $k+1$, and the impact of adding the edge re-evaluated against the new values, $k+1$ and $g(k+1)$. This final step of augmenting the cap and re-evaluating the impact is iterated until either k increases sufficiently to accept the edge or $g(k)$ decreases sufficiently that the edge can be rejected. Asymptotically, the fraction of accepted edges is $\lim_{k\to\infty} g(k) = \alpha$.

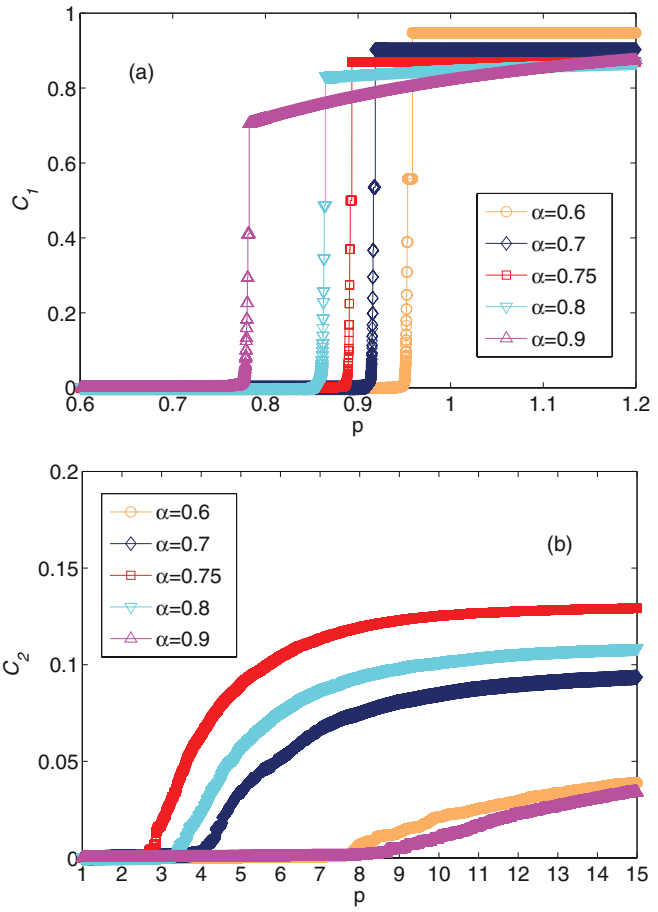

FIG. 1. (Color online) Typical evolution of the BFW model. (a) Fraction of nodes in the largest component, $C_1 = |C_1|/N$, as a function of edge density $p \equiv t/N$, for different values of α, showing a discontinuous phase transition at a location dependent on the value of α. As derived herein, for $\alpha > \alpha_c$ the size of C_1 increases in the supercritical regime. (b) Fraction of nodes in the second largest component, $C_2 = |C_2|/N$, as a function of p for $\alpha = 0.75,0.8,0.7,0.6,0.9$ from left to right, showing an instantaneous peak when C_1 emerges followed later by a continuous phase transition. The extent of delay between the discontinuous emergence of C_1 and the continuous emergence of C_2 depends in the value of α. The system size is $N = 10^6$.

Stating the BFW algorithm in detail requires some notation. Let k denote the cap size, N denote the number of nodes, u denote the total number of edges sampled, A denote the set of accepted edges, and $t = |A|$ denote the number of accepted edges. At each step u, an edge e_u is sampled uniformly at random from the complete graph generated by the N nodes

and evaluated by the following algorithm, stopping once a specified number of edges, ωN, have been accepted:

Repeat until $u = \omega N$
{
Set l = size of largest component in $A \cup \{e_u\}$
if $(l \leqslant k)$ {
$A \leftarrow A \cup \{e_u\}$
$u \leftarrow u + 1$ }
else if $(t/u < g(k))\{k \leftarrow k + 1$ }
else { $u \leftarrow u + 1$ }
}

It has been shown in Ref. [38] that the percolation transition of the order parameter $|C_1|/N := C_1$, defined as the fraction of nodes in the largest component, is discontinuous in the thermodynamic limit for $\alpha \in (0,0.97]$ [see, e.g., Fig. 1(a)]. This holds regardless of whether we sample uniformly at random all edges from the complete graph or sample only edges not yet existing in the graph [38]. (The former allows intracomponent edges including multiple edges and self-edges.) Here we provide additional numerical evidence for the discontinuous transition by examining three quantities: the largest jump in C_1 resulting from adding one edge, denoted as $\Delta C_{\max}$, order parameter C_1 immediately after the largest jump, denoted as P_∞, and the maximum in the second moment of the relative-size distribution of components, excluding the contribution of the largest component,

$$M_2' = M_2 - C_1^2, \tag{1}$$

where $M_2 = \sum_i C_i^2$ and C_i is the relative size of component i. If $\Delta C_{\max}, P_\infty, M_2'$ converge to some positive constant in the thermodynamic limit, the transition is discontinuous while they vanish for continuous phase transitions [21,26,28,37]. We observe $\Delta C_{\max}, P_\infty$, and M_2' are all asymptotically independent of system sizes within error bars which are shown in Figs. 2(a)–2(c) respectively. For large size systems and differing values of α, we obtain the asymptotic values of $\Delta C_{\max}$, P_∞, and M_2' for $\alpha = 0.6,0.7,0.8,0.9,0.95$, respectively (Table I). These numerical results indicate that the percolation transition is discontinuous for the range studied here, $\alpha \in [0.6,0.95]$.

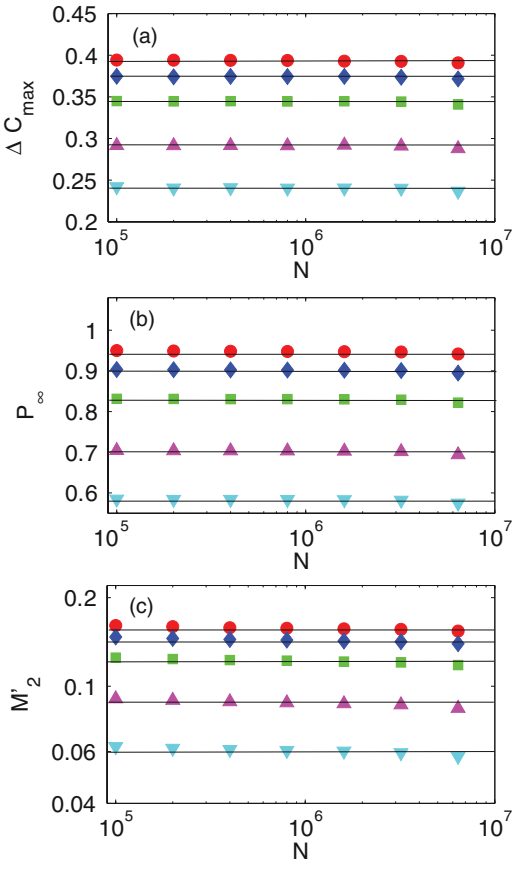

FIG. 2. (Color online) (a) The largest jump in the size of C_1 resulting from one edge as a function of system sizes for $\alpha = 0.6,0.7,0.8,0.9,0.95$ ordered from top to bottom. (b) The order parameter P_∞, which is C_1 immediately after the largest jump of C_1, as a function of system sizes for $\alpha = 0.6,0.7,0.8,0.9,0.95$ from top to bottom. (c) The maximum of the second moment of the cluster-size distribution M_2' as a function of system size for $\alpha = 0.6,0.7,0.8,0.9,0.95$ from top to bottom. All the quantities in (a), (b), and (c) are asymptotically independent of system sizes and the solid lines are the mean values. These results indicate that the percolation transitions are discontinuous. Each datum is averaged over 500 realizations.

TABLE I. Summary of numerical results showing discontinuous phase transitions in the order parameter C_1.

α	$\Delta C_{\max}$	P_∞	M_2'
0.6	0.391 ± 0.005	0.947 ± 0.004	0.154 ± 0.005
0.7	0.374 ± 0.006	0.901 ± 0.005	0.139 ± 0.006
0.8	0.344 ± 0.005	0.829 ± 0.004	0.118 ± 0.006
0.9	0.291 ± 0.005	0.702 ± 0.005	0.084 ± 0.006
0.95	0.240 ± 0.006	0.582 ± 0.005	0.057 ± 0.008

To estimate the percolation threshold, we implement the numerical methods proposed in Refs. [28,37]. We measure the edge density $p_{c,1}(N)$ at which the largest jump in the size of C_1 occurs and the edge density $p_{c,2}(N)$ at which M_2' attains maximum for different system sizes N. Extrapolating these estimators in thermodynamic limit, we obtain $p_c = 0.948 \pm 0.007, 0.915 \pm 0.008, 0.862 \pm 0.007, 0.780 \pm 0.007, 0.711 \pm 0.006$ for $\alpha = 0.6,0.7,0.8,0.9,0.95$, respectively. These results indicate the percolation threshold for the emergence of a giant component is larger for smaller α. We further observe asymptotic power law relation between $|p_{c,i} - p_c| (i = 1,2)$ and system size N. In particular, $|p_{c,i} - p_c| \sim N^{-\delta}$ with $\delta = 0.3 \pm 0.1, 0.4 \pm 0.1, 0.4 \pm 0.1, 0.5 \pm 0.1, 0.5 \pm 0.1$ for $\alpha = 0.6,0.7,0.8,0.9,0.95$, respectively. The exponent $\delta = 0.5 \pm 0.1$ for $\alpha = 0.9,0.95$ is the same as what is observed for BFW model ($\alpha = 0.5$) on a square lattice within error bars [37].

III. GROWTH CESSATION OF THE LARGEST COMPONENT

The discontinuous transition of the order parameter C_1 has been substantiated [38] and the underlying mechanism accounting for the discontinuous transition has been identified [40]. However, the behavior of C_1 after the largest jump (i.e., in supercritical regime) has not been studied previously. Here we

study C_1 for values of the edge density $p \in [0,10]$ for different system sizes. Interestingly we observe that C_1 stops increasing either immediately after the largest jump of C_1 or at some delayed point dependent on the specific $\alpha \in [0.6,0.95]$. This growth cessation of the largest component in the supercritical regime has however, not been reported in other models in which any edge from the complete graph is allowed to be sampled.

Using the notation in Sec. II, t denotes the number of accepted edges, and thus t/N is the edge density (also denoted throughout by the shorthand $p \equiv t/N$). Let us denote t_c as the point where the largest jump of C_1 occurs and k_c as the value of stage k at t_c. Also denote k_{final} as the final value when k stops increasing and $t(k_{\text{final}})$ as the point where k stops increasing. We measure $k(t_c), k_{\text{final}}, t_c/N, t(k_{\text{final}})/N$ for different α in a system of size $N = 10^6$. Figure 3(a) shows when $\alpha < \alpha_c \approx 0.763$, $k(t_c)$ and k_{final} overlap and both decrease with α. When $\alpha > \alpha_c$ however, $k(t_c)$ keeps on decreasing while k_{final} increases with α. Therefore k_{final}/N reaches a minimum at $\alpha = \alpha_c$. Let $\Delta k/N = (k_{\text{final}} - k(t_c))/N$ and Fig. 3(b) shows $\Delta k/N \sim N^{-1.07}, N^{-0.93}$ for $\alpha = 0.76, 0.75$, respectively, indicating $\Delta k/n \to 0$ as $n \to \infty$. For $\alpha = 0.77$ however, $\Delta k/N$ converges to some positive constant. More precise investigation detailed below shows the transition point $\alpha_c = 0.763 \pm 0.002$. Figure 3(c) shows t_c/N and $t(k_{\text{final}})/N$ overlap when $\alpha < \alpha_c \approx 0.763$ and there is a finite gap between them once $\alpha > \alpha_c$. We observe that $t(k_{\text{final}})$ reaches a minimum at α_c. Let $\Delta t/N = (t(k_{\text{final}}) - t_c)/N$ and in Fig. 3(d) $\Delta t/N$ is plotted as a function of N for $\alpha = 0.75, 0.76, 0.77$ where $\Delta t/N \sim N^{-1.03}, N^{-0.82}$ for $\alpha = 0.76, 0.75$, respectively, but asymptotically converges to some positive constant for $\alpha = 0.77$. This numerical result shows the same transition point at $\alpha_c \approx 0.763$.

To understand the underlying mechanism accounting for the fact that the stage k and the size of the largest component stops increasing in the supercritical regime, it is useful to measure $P(k,t,N)$, defined as the probability of sampling a random edge that keeps $C_1 N \leqslant k$ if it is added at step t in a system of size N. If $\lim_{N\to\infty} P(k,t,N) \geqslant \lim_{k\to\infty} g(k) = \alpha$ always holds for $t > t_c$ where $k \sim \mathcal{O}(N)$, the fraction of accepted edges over total sampled edges t/u quickly converges to some value larger than α, so we can always discard an edge that would increase C_1, thus stage stops increasing. However, if $\lim_{N\to\infty} P(k,t,N) < \alpha$, the stage k keeps on increasing until

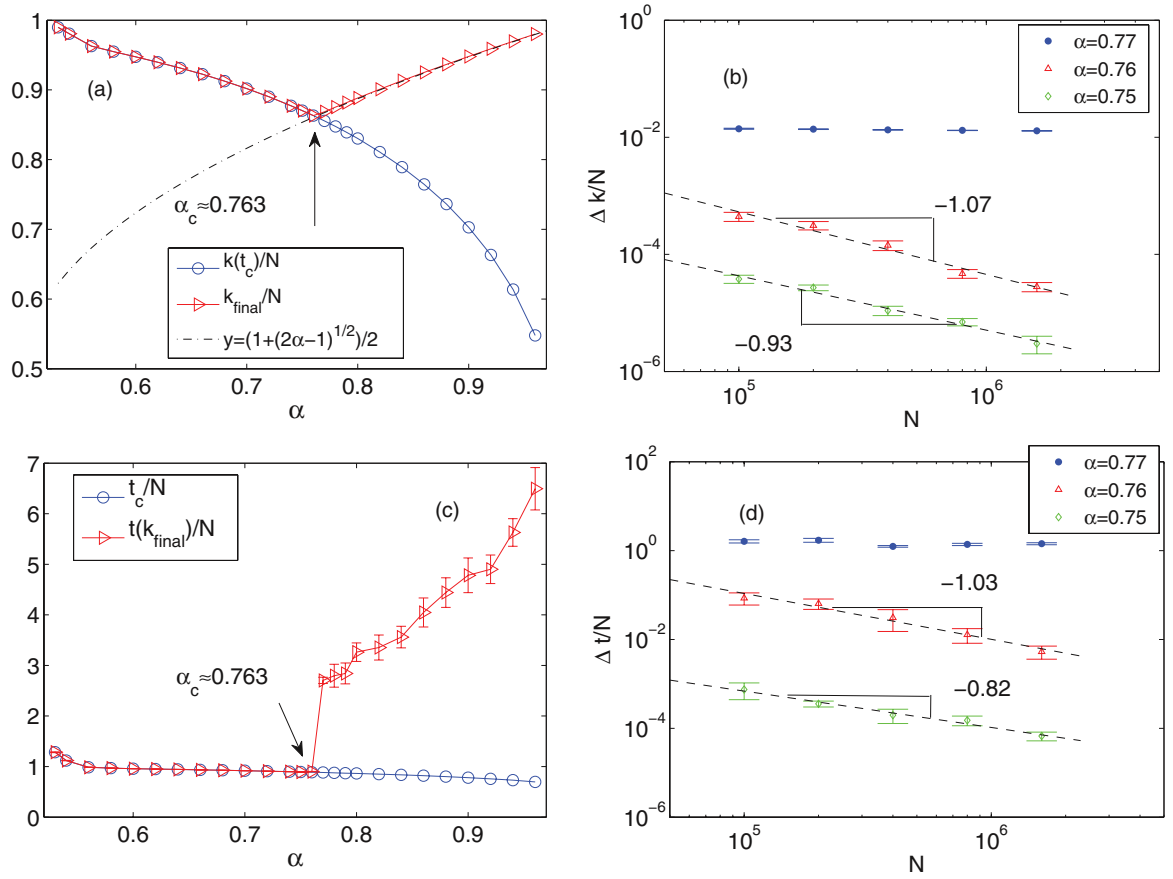

FIG. 3. (Color online) System size is $N = 10^6$ for (a),(c). (a) Behavior of the cap k versus α specifically measuring $k(t_c)/N$ (blue circles) the value at the discontinuous emergence of C_1, and k_{final}/N (red triangles) the value when k stops increasing. Both lines intersect the function derived in Eq. (4), $y = (1 + (2\alpha - 1)^{1/2})/2$, at the same point $\alpha_c \approx 0.763$. (b) $\Delta k/N$ versus system size for $\alpha = 0.75, 0.76, 0.77$ (ordered bottom to top), showing $\Delta k/N$ converges to 0 for $\alpha = 0.75, 0.76$ while it converges to a positive constant for $\alpha = 0.77$. Further analysis shows $\alpha = 0.763 \pm 0.002$ is the transition point between the behaviors. (c) t_c/N and $t(k_{\text{final}})/N$ as a function of α. (d) $\Delta t/N$ versus system size for $\alpha = 0.75, 0.76, 0.77$ (ordered bottom to top), showing $\Delta t/N$ converges to 0 asymptotically for $\alpha = 0.75, 0.76$ while it asymptotically converges to some positive constant for $\alpha = 0.77$. More detailed analysis shows $\alpha = 0.763 \pm 0.002$ is the transition point between the two behaviors.

the following condition holds at $t = t(k_{\text{final}})$

$$\lim_{N\to\infty} P(k,t,N) = \alpha. \tag{2}$$

We measure $k(t_c)/N$ and k_{final}/N with system sizes $N = 10^6$ for over 100 realizations. We find that at the point where the largest jump of C_1 occurs, namely t_c/N, for all $\alpha \in [0.6,0.95]$, $k(t_c)/N = C_1 > 0.5$ averaged over 1000 realizations. Due to this fact, once $t > t_c$, the growth of C_1 can only occur due to the mechanism of direct growth [21], in particular, the edge connecting the largest component and another smaller component results in the growth of C_1. Therefore, the probability of sampling a random edge which leads to the growth of C_1 is $2(1 - C_1)C_1$ and thus, $P(k,t,N)$ satisfies

$$\lim_{N\to\infty} P(k,t,N) = 1 - 2(1 - C_1)C_1. \tag{3}$$

Combining Eqs. (2) and (3), we obtain C_1 at $t(k_{\text{final}})$ for infinite system

$$C_1 = \frac{1+\sqrt{2\alpha-1}}{2}. \tag{4}$$

Figure 3(a) shows the dashed line of Eq. (4) intersects $k(t_c)/N$ and k_{final}/N at the same point $\alpha_c = 0.763$ within error bars for system size $N = 10^6$. For $\alpha < \alpha_c$, $k(t_c)/N > \frac{1+\sqrt{2\alpha-1}}{2}$ (blue circles lie above the dashed line), and $P(k,t_c,N) > \alpha$. Therefore the stage k stops increasing immediately after the largest jump of C_1 and k_{final}/N is almost the same as $k(t_c)/N$ (blue circles and red triangles overlap). However, for $\alpha > \alpha_c$, $k(t_c)/N < \frac{1+\sqrt{2\alpha-1}}{2}$(blue circles lie below the dashed line). Therefore both the stage k and C_1 increase until Eq. (4) holds (red triangles and the dashed line overlap).

IV. CONTINUOUS TRANSITION OF THE SECOND LARGEST COMPONENT

The size of the largest component stops increasing at the point $t(k_{\text{final}})/N$ (which is either at the discontinuous phase transition point or in the supercritical regime, dependent on the value of α). Yet, the second largest component continues growing at this point. Two natural and interesting questions follow. Is there a second giant component emerging at some step $t > t(k_{\text{final}})$? If such percolation transition occurs, is it a discontinuous phase transition as we find for the order parameter C_1? To answer these questions, we first numerically measure C_2 as a function of the edge density $p \equiv t/N$ for

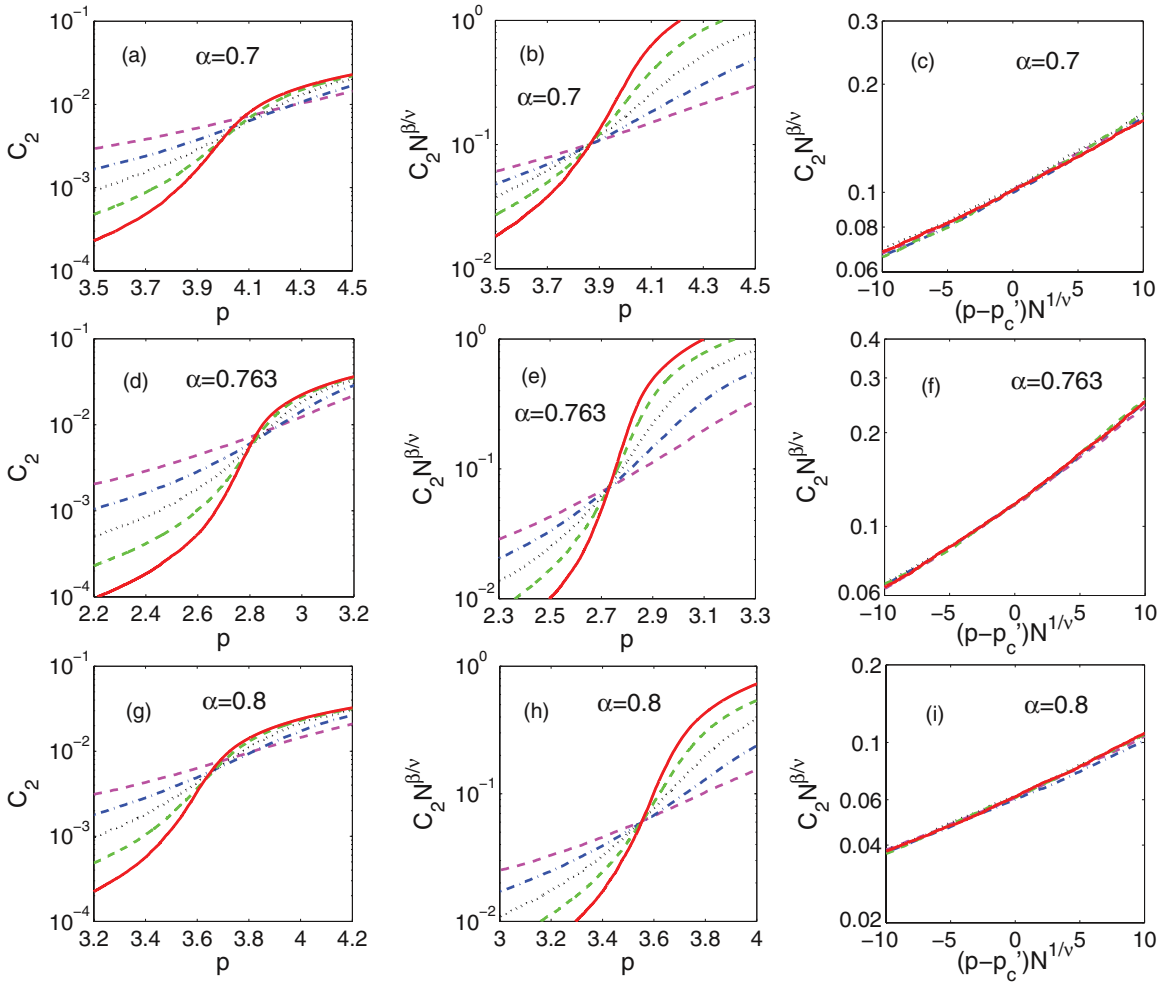

FIG. 4. (Color online) In (a), (d), (g), fraction of nodes in the second largest component, C_2 is plotted as a function of edge density p for $\alpha = 0.7,0.763,0.8$, respectively. (b), (e), (h) show their rescaling $C_2N^{\beta/\bar{\nu}}$, respectively. (c), (f), (i) show $C_2N^{\beta/\bar{\nu}}$ versus $(p - p_c')N^{1/\bar{\nu}}$, indicating the validity of Eq. (7). The system size goes from $N = 20\,000$ (the dashed magenta line) to $1\,620\,000$ (the solid red line) via successive doubling.

$\alpha = 0.6,0.65,0.7,0.75,0.8,0.85,0.9$. As shown in Fig. 1(b), we see C_2 (the fractional size of component C_2) spike instantaneously at the first discontinuous transition, then it disappears and we observe a seemingly continuous percolation transition when C_2 again emerges at some point in the supercritical regime.

To investigate the continuous nature of percolation transition of C_2, we make use of finite size scaling [51]. If a phase transition is continuous, every variable X is believed to be scale independent and obeys the following finite size scaling form near the percolation threshold p_c

$$X = N^{-\theta/\nu} F[(p - p_c)N^{1/\nu}],$$

where θ and ν are critical exponents, N is the system size, and F is a universal function. If the dimension of the system d exceeds the upper critical dimension d_c the finite-size scaling form for a variable X is assumed to satisfy

$$X = N^{-\theta/\bar{\nu}} F[(p - p_c)N^{1/\bar{\nu}}], \tag{5}$$

where $\bar{\nu} = d_c \nu_m$, and ν_m is the mean-field value of ν. As a result, X follows a power law at $p = p_c$, $X \sim N^{-\theta/\bar{\nu}}$. Random networks display a mean-filed type critical behavior [52] and lack any space dimensionality, essentially, $d = \infty$. Here we consider two variables in the percolation process: the fraction of nodes in the second largest component C_2 and the susceptibility χ. The susceptibility χ is defined as the standard deviation of the size of the second largest component

$$\chi = N\sqrt{\langle C_2^2 \rangle - \langle C_2 \rangle^2}. \tag{6}$$

We assume that C_2 and χ obey the following scaling relations:

$$C_2 = N^{-\beta/\bar{\nu}} F^{(1)}[(p - p_c')N^{1/\bar{\nu}}], \tag{7}$$

$$\chi = N^{\gamma/\bar{\nu}} F^{(2)}[(p - p_c')N^{1/\bar{\nu}}], \tag{8}$$

where $F^{(1)}$ and $F^{(2)}$ are different universal functions (however, they are related to each other), p_c' denotes the percolation threshold of the second phase transition, and $\beta, \gamma, \bar{\nu}$ are critical exponents characterizing the transition. We can deduce from the definition of χ [Eq. (6)] and the scaling relations in Eqs. (7) and (8) at $p = p_c'$

$$\beta/\bar{\nu} = 1 - \gamma/\bar{\nu}. \tag{9}$$

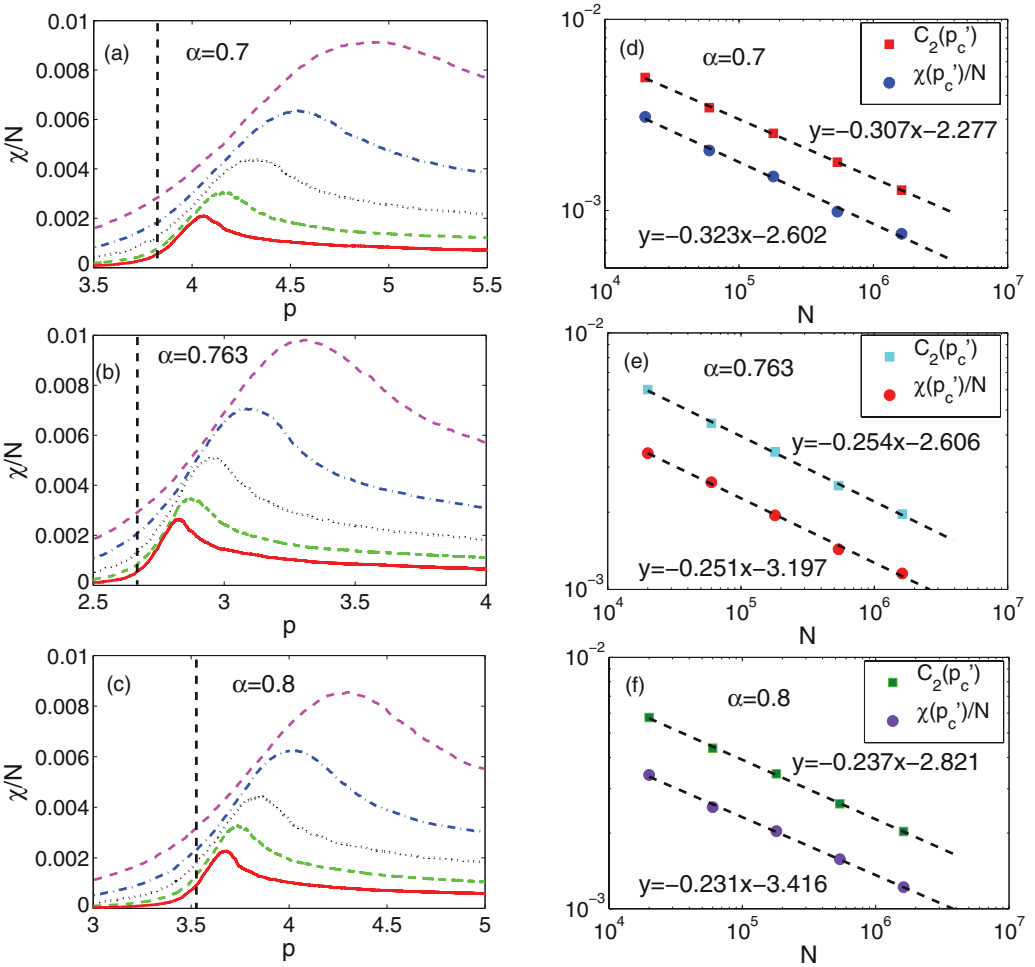

FIG. 5. (Color online) In (a), (b), (c), χ/N is plotted as a function of p for $\alpha = 0.7,0.763,0.8$, respectively, showing the peak of χ/N moves leftward as system size increases. The dashed lines are the percolation threshold obtained from numerical simulation through Eq. (8). The peaks of χ/N is moving leftward to the percolation threshold p_c' which indicates the continuous nature of the second phase transition. In (d), (e), (f), C_2 and χ/N at the percolation threshold p_c' is plotted as a function of system sizes for $\alpha = 0.7,0.763,0.8$, respectively. The system size goes from $N = 20\,000$ (the dashed magenta line) to $1\,620\,000$ (the solid red line) via successive doubling.

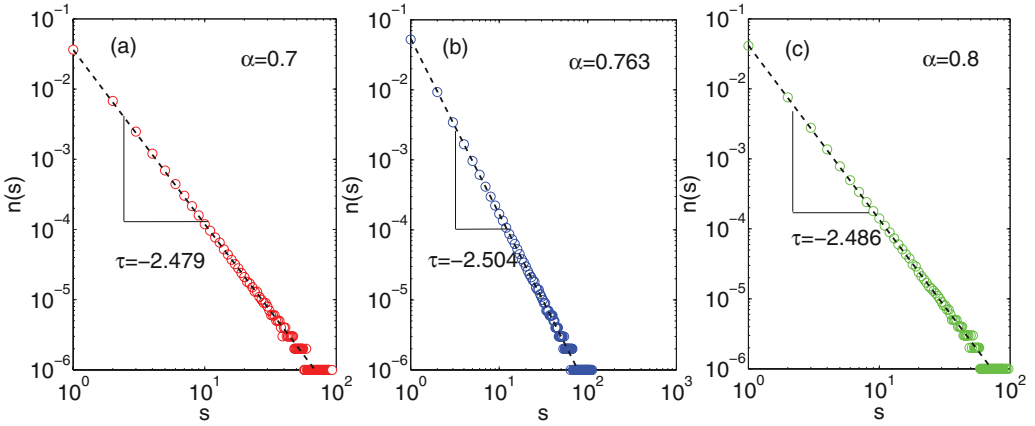

FIG. 6. (Color online) Component size distribution $n(s)$ at the percolation threshold p_c' for $\alpha = 0.7$ (a), 0.763 (b), 0.8 (c), respectively.

Since Eqs. (7) and (8) imply that the curves of $N^{\beta/\bar{\nu}}C_2$ vs p and $N^{-\gamma/\bar{\nu}}\chi$ vs p for different systems sizes cross at a single point at $p = p_c'$, both the relative size of the second largest component C_2 and the susceptibility χ can be used for the determination of percolation threshold p_c'. More precisely, we implement the minimization technique in Ref. [53]. For each system size N, we use Monte Carlo data for C_2 vs p and χ/N vs p to create functions $g_N = N^{\beta/\bar{\nu}}C_2$ and $l_N = N^{-\gamma/\bar{\nu}}\chi$, respectively. The value of p that minimizes the objective function $P = \sum_{Ni<Nj}(g_{Ni} - g_{Nj})^2$ is the estimation of percolation threshold p_c'. Similarly, the value of p which minimizes the objective function $Q = \sum_{Ni<Nj}(l_{Ni} - l_{Nj})^2$ is an alternative way to estimate p_c'. In our following numerical simulations, we find a perfect agreement within error bars between the two different methods.

In Figs. 4(a), 4(d), and 4(g), we plot the order parameter C_2 as a function of edge density p, for $\alpha = 0.7,0.763,0.8$ in the BFW model, respectively. Five curves in each figure stand for Monte Carlo data averaged over 1000 realizations for five different system sizes, namely $N = 20\,000,60\,000,180\,000,540\,000,1\,620\,000$. To identify the percolation threshold p_c' of C_2 and two scaling exponents $\beta/\bar{\nu},\gamma/\bar{\nu}$, we first implement the minimization technique in the objective function P. Figures 4(b), 4(e), and 4(h) show that all curves of $C_2N^{\beta/\bar{\nu}}$ vs p cross at a single percolation transition point $p_c' = 3.865 \pm 0.005,3.555 \pm 0.005,2.725 \pm 0.003$ for $\alpha = 0.7,0.763,0.8$, respectively. The corresponding exponent ratios $\beta/\bar{\nu}$ are $0.31 \pm 0.03,0.25 \pm 0.04,0.24 \pm 0.04$ for $\alpha = 0.7,0.763,0.8$, respectively. In Figs. 4(c), 4(f), and 4(i), the data collapses show the profiles of the universal scaling function $F^{(1)}$ of Eq. (7), where we find the exponent $1/\nu = 0.36 \pm 0.01,0.36 \pm 0.01,0.37 \pm 0.01$ for $\alpha = 0.7,0.763,0.8$, respectively.

In Figs. 5(a), 5(b), and 5(c), χ/N is plotted as a function of p, where the dashed lines show the location of the percolation threshold through minimization of the objective function Q. We find that percolation threshold obtained through minimization technique in the objective functions P and Q show perfect agreement within error bars. Figures 5(d)–5(f) display C_2 and χ/N at $p = p_c'$ as a function of system size N for $\alpha = 0.7,0.763,0.8$, respectively. The slope of dashed lines which are the best fit of points represent the exponent ratios $-\beta/\bar{\nu}$ and $\gamma/\bar{\nu} - 1$ in scaling relations Eqs. (7) and (8). We obtain that $1 - \gamma/\bar{\nu} = 0.32 \pm 0.03,0.25 \pm 0.04,0.23 \pm 0.05$ for $\alpha = 0.7,0.763,0.8$, respectively, which agree with the corresponding exponent ratios $\beta/\bar{\nu}$. Therefore the validity of Eq. (9) has been verified. The exponent ratios $\beta/\bar{\nu},\gamma/\bar{\nu}$ for $\alpha = 0.7$ are the same within error bars as observed for ER [17], suggesting they belong to the same universality class. The measurement of exponents β,γ and $\bar{\nu}$ verify the fact that the percolation transition is continuous.

Next, we numerically measure at the percolation threshold p_c', the number of components of size s divided by the number of nodes N, denoted as $n(s)$. Figures 6(a)–6(c) show that $n(s)$ follow a power law distribution for $\alpha = 0.7,0.763,0.8$ with respective scaling exponent $\tau = 2.48 \pm 0.01,2.50 \pm 0.01,2.49 \pm 0.01$, which is further evidence for a continuous phase transition. The continuous phase transition of the second largest component is a consequence of a relatively large value of the cap k throughout the continuous growth process of C_2. This stands in contrast to the subcritical regime for C_1 where small values of k keep components similar in size by the mechanism of growth by overtaking.

The ratios of the scaling exponents $\beta/\bar{\nu},\gamma/\bar{\nu}$, and the percolation threshold p_c' are measured by minimization technique with results shown in Table II. For $\alpha \in [0.6,0.95]$ we find

TABLE II. Summary of numerical results obtained from minimization technique.

α	0.6	0.65	0.68	0.7	0.72	0.75	0.763(α_c)	0.8	0.85	0.9
$\beta/\bar{\nu}$	0.26(4)	0.31(4)	0.30(3)	0.31(3)	0.27(3)	0.30(3)	0.25(4)	0.24(5)	0.28(4)	0.22(5)
$\gamma/\bar{\nu}$	0.74(4)	0.68(4)	0.68(1)	0.68(3)	0.73(3)	0.68(3)	0.75(4)	0.77(5)	0.72(4)	0.78(5)
τ	2.50 (1)	2.48(2)	2.49(2)	2.48(1)	2.49(1)	2.49(2)	2.50(1)	2.49(1)	2.46(2)	2.48(2)
p_c'	7.595(6)	5.320(5)	4.385(5)	3.865(5)	3.455(4)	2.860(4)	2.725(3)	3.555(5)	5.215(5)	8.647(7)

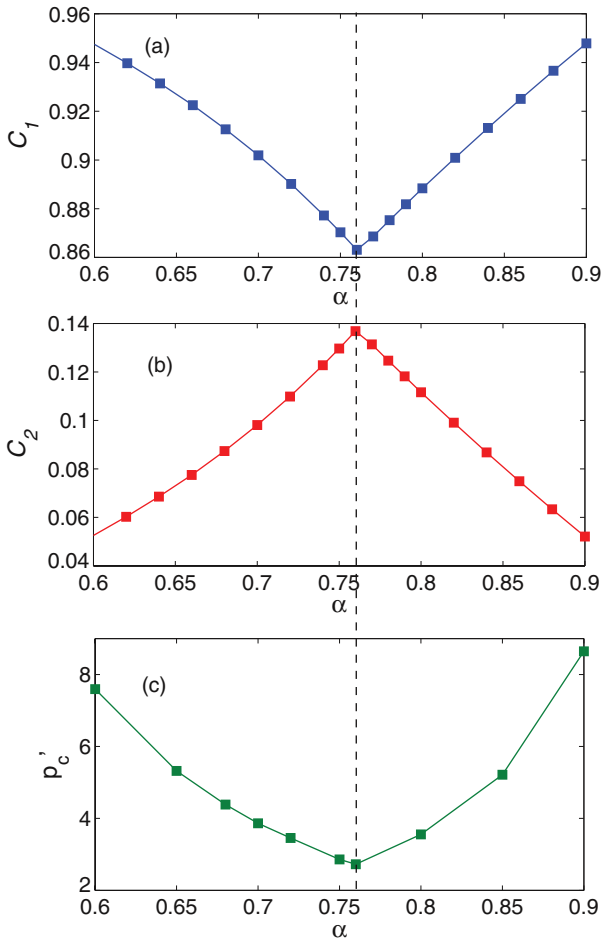

FIG. 7. (Color online) (a) The asymptotic fraction of nodes in the largest component is plotted as a function of α. (b) The asymptotic fraction of nodes in the second largest component is plotted as a function of α. (c) The percolation threshold p_c' of the second phase transition is plotted as a function of α. The minimal values of C_1 and p_c', the maximal value of C_2 are obtained at the same critical point $\alpha_c = 0.763 \pm 0.001$, marking also the point with the minimal delay between the emergence of C_1 and C_2.

strong numerical evidence that the percolation transition is indeed continuous. We also deduce from Table II that the minimal percolation threshold of the order parameter C_2 is obtained for $\alpha_c = 0.763 \pm 0.002$ as also shown explicitly in Fig. 7(c). This observation shows perfect agreement with the location where $t(k_{\text{final}})$ and k_{final}/N attain their minimums [Fig. 3(a)]. The underlying mechanism which accounts for the minimal percolation threshold obtained at $\alpha_c = 0.763 \pm 0.002$, is actually related with the behavior of C_1 (or stage k) in supercritical regime. Since if $\alpha < \alpha_c$, both $k(t_c)/N$ and t_c/N decrease with α from numerical results obtained in Sec. III, the emergence of the second giant component is earlier for larger α. However, if $\alpha > \alpha_c$, C_1 keeps on augmenting after t_c/N and a finite fraction of edges is added before $t(k_{\text{final}})/N$. Therefore the competition of edges enhancing the largest component and the second largest component delays the onset of the second giant component. In particular, the emergence of the second giant component is more delayed for larger α if $\alpha > \alpha_c$. Thus we observe the minimal percolation threshold of the order parameter C_2 is derived for $\alpha_c = 0.763 \pm 0.002$.

V. SUMMARY AND DISCUSSION

In this paper, we have analyzed the BFW model in the regime $\alpha \in [0.6,0.95]$ where only one giant component appears in a discontinuous phase transition. The growth cessation of the largest component in the supercritical regime results in the emergence of a second giant component at some delayed time. We have carried out finite-size scaling to study the critical behavior of the second phase transition and the results establish that the transition is continuous. We have also established that there exists an interesting inflection point at $\alpha_c = 0.763 \pm 0.002$ that is related to many properties of the system. As derived in Eq. (4), for $\alpha < \alpha_c$, C_1 stops growing the instant it emerges, whereas for $\alpha > \alpha_c$, C_1 grows in the supercritical regime. As shown in Fig. 7, at α_c the asymptotic size of C_1 is minimized, that of C_2 is maximized, and the delay between the emergence of C_1 and C_2 is minimized.

There is much recent interest in understanding the formation mechanism of multiple giant components in percolation [38,40,54,55]. In Refs. [38,40], the modified BFW model with $\alpha < 0.52$ exhibits multiple giant components which emerge in a discontinuous transition. The underlying mechanisms responsible for the formation of multiple giant components are (i) the domination of overtaking processes in the growth of C_1 which result in the coexistence of many large components in the critical window, and (ii) the dominance of the sampling of intracomponent edges in the supercritical region which avoids merging the giant components. In Ref. [54], the so called *multi-ER* model shows multiple giant components appear in a continuous transition. The formation of multiple giant components is attributed to the relatively low probability for merger of large components in the critical window. In this paper, the BFW model with $\alpha \in [0.6,0.95]$ provides a novel formation mechanism resulting in multiple giant components, which is the growth cessation of C_1 in supercritical regime resulting in the emergence of a second giant component.

The hybrid of continuous and discontinuous phase transitions observed in the modified BFW model studied here is an unusual characteristic in classical statistical mechanics of critical phenomena. In a recent study, a competitive percolation model called the Nagler-Tiessen-Gutch model (NTG) [50] has been proposed in which three nodes are randomly sampled at each step and an edge is added between two nodes that reside in components most similar in size. The NTG model undergoes both continuous and discontinuous phase transitions as well. However, there is a different main feature between the NTG model and the modified BFW model with $\alpha \in [0.6,0.9]$. In the NTG model, the double giant components would merge infinitely many times in the supercritical regime, leading to infinite discontinuous transitions of C_1 and infinite continuous transitions of C_2 while in the modified BFW model there are asymptotically stable double giant components that never merge.

It is a longstanding challenge to substantiate the discontinuity of phase transition. Here we have investigated the discontinuity of phase transition of the BFW model by estimating the asymptotic values of ΔC, P_∞, and M_2' through

numerical simulations. It would be interesting to understand the dependence of ΔC, P_∞, and M_2' on α in the function of $g(k)$ in a rigorous analytical manner, which will be our future study.

ACKNOWLEDGMENTS

We are grateful to Robert Ziff for useful comments. This work was supported by the Defense Threat Reduction Agency, Basic Research Award No. HDTRA1-10-1-0088, the Army Research Laboratory under Cooperative Agreement No. W911NF-09-2-0053, the 973 National Basic Research Program of China (Grant No. 2005CB321902), and the 973 National Basic Research Program of China (No. 2013CB329602), the National Natural Science Foundation of China under Grant Nos. 61232010 and 61202215.

[1] S. H. Strogatz, Nature **410**, 268 (2001).
[2] M. E. J. Newman, D. J. Watts, and S. H. Strogatz, Proc. Natl Acad. Sci **99**, 2566 (2002).
[3] C. Song, S. Havlin, and H. A. Makse, Nat. Phys. **2**, 275 (2006).
[4] S. V. Buldyrev, R. Parshani, G. Paul, H. E. Stanley, and S. Havlin, Nature **464**, 1025 (2010).
[5] J. Kim, P. L. Krapivsky, B. Kahng, and S. Redner, Phys. Rev. E **66**, 055101 (2002).
[6] H. D. Rozenfeld, L. K. Gallos, and H. A. Makse, Eur. Phys. J. B **75**, 305 (2010).
[7] Cristopher Moore and M. E. J. Newman, Phys. Rev. E **61**, 5678 (2000).
[8] M. A. Serrano and M. Boguñá, Phys. Rev. Lett. **97**, 088701 (2006).
[9] S. N. Dorogovtsev, A. V. Goltsev, and J. F. F. Mendes, Rev. Mod. Phys. **80**, 1275 (2008).
[10] R. Parshani, S. Carmi, and S. Havlin, Phys. Rev. Lett. **104**, 258701 (2010).
[11] M. Ausloos and R. Lambiotte, Physica A **382**, 1621 (2007).
[12] Carlos P. Roca, Moez Draief, and Dirk Helbing, arXiv:1101.0775.
[13] P. Erdös and A. Rényi, Publ. Math. Inst. Hung. Acad. Sci. **5**, 17 (1960).
[14] D. Achlioptas, R. M. D'Souza, and J. Spencer, Science **323**, 1453 (2009).
[15] Y. S. Cho, J. S. Kim, J. Park, B. Kahng, and D. Kim, Phys. Rev. Lett. **103**, 135702 (2009).
[16] F. Radicchi and S. Fortunato, Phys. Rev. Lett. **103**, 168701 (2009).
[17] F. Radicchi and S. Fortunato, Phys. Rev. E **81**, 036110 (2010).
[18] R. M. Ziff, Phys. Rev. Lett. **103**, 045701 (2009).
[19] R. M. Ziff, Phys. Rev. E **82**, 051105 (2010).
[20] R. A. da Costa, S. N. Dorogovtsev, A. V. Goltsev, and J. F. F. Mendes, Phys. Rev. Lett. **105**, 255701 (2010).
[21] J. Nagler, A. Levina, and M. Timme, Nat. Phys. **7**, 265 (2011).
[22] O. Riordan and L. Warnke, Science **333**, 322 (2011).
[23] P. Grassberger, C. Christensen, G. Bizhani, S.-W. Son, and M. Paczuski, Phys. Rev. Lett. **106**, 225701 (2011).
[24] H. K. Lee, B. J. Kim, and H. Park, Phys. Rev. E **84**, 020101(R) (2011).
[25] Y. S. Cho, B. Kahng, and D. Kim, Phys. Rev. E **81**, 030103(R) (2010).
[26] N. A. M. Araújo and H. J. Herrmann, Phys. Rev. Lett. **105**, 035701 (2010).
[27] A. A. Moreira, E. A. Oliveira, S. D. S. Reis, H. J. Herrmann, and J. S. Andrade, Phys. Rev. E **81**, 040101(R) (2010).
[28] K. J. Schrenk, N. A. M. Araújo, and H. J. Herrmann, Phys. Rev. E **84**, 041136 (2011).
[29] W. Choi, S.-H. Yook, and Y. Kim, Phys. Rev. E **84**, 020102(R) (2011).
[30] Y. S. Cho and B. Kahng, Phys. Rev. E **84**, 050102(R) (2011).
[31] Y. S. Cho, Y. W. Kim, and B. Kahng, J. Stat. Mech. (2012) P10004.
[32] K. Panagiotou, R. Spőhel, A. Steger, and H. Thomas, Elec. Notes in Discrete Math. **38**, 699 (2011).
[33] S. Boettcher, V. Singh, and R. M. Ziff, Nature Communications **3**, 787 (2012).
[34] G. Bizhani, M. Paczuski, and P. Grassberger, Phys. Rev. E **86**, 011128 (2012).
[35] L. Cao and J. M. Schwarz, Phys. Rev. E **86**, 061131 (2012).
[36] Y. S. Cho and B. Kahng, Phys. Rev. Lett. **107**, 275703 (2011).
[37] K. J. Schrenk, A. Felder, S. Deflorin, N. A. M. Araújo, R. M. D'Souza, and H. J. Herrmann, Phys. Rev. E **85**, 031103 (2012).
[38] W. Chen and R. M. D'Souza, Phys. Rev. Lett. **106**, 115701 (2011).
[39] T. Bohman, A. Frieze, and N. C. Wormald, Random Structures & Algorithms **25**, 432 (2004).
[40] W. Chen, Z. Zheng, and R. M. D'Souza, Europhys. Lett. **100**, 66006 (2012).
[41] M. Bengtsson and S. Kock, J. Bus. Ind. Mark. **14**, 178 (1999).
[42] S. A. Frank, Evolution: Int. J. Org. Evol. **57**, 693 (2003).
[43] J. Hirshleifer, Am. Econ. Rev. **68**, 238 (1978).
[44] J. Spencer, Not. Am. Math. Soc. **57**, 720 (2010).
[45] E. Ben-Naim and P. L. Krapivsky, J. Phys. A **38**, L417 (2005).
[46] A. Asztalos and Z. Toroczkai, Europhys. Lett. **92**, 50008 (2010).
[47] R. M. Anderson and R. M. May, *Infectious Diseases in Humans* (Oxford University Press, Oxford, 1992).
[48] S. S. Manna and A. Chatterjee, Physica A **390**, 177 (2011).
[49] O. Riordan and L. Warnke, Phys. Rev. E **86**, 011129 (2012).
[50] J. Nagler, T. Tiessen, and H. W. Gutch, Phys. Rev. X **2**, 031009 (2012).
[51] D. P. Landau and K. Binder, *A Guide to Monte Carlo Simulations in Statistical Physics* (Cambridge University Press, Cambridge, England, 2000).
[52] H. Hong, M. Ha, and H. Park, Phys. Rev. Lett. **98**, 258701 (2007).
[53] N. Bastas, K. Kosmidis, and P. Argyrakis, Phys. Rev. E **84**, 066112 (2011).
[54] Y. Zhang, W. Wei, B. Guo, R. Zhang, and Z. Zheng, Phys. Rev. E **86**, 051103 (2012).
[55] R. Zhang, W. Wei, B. Guo, Y. Zhang, and Z. Zheng, Physica A **392**, 1232 (2013).